*Proceedings of the 20th International Conference on Soil Mechanics and Geotechnical Engineering– Rahman and Jaksa (Eds)*


# A novel miniature tunnel boring machine for use in a geotechnical centrifuge

**CJ Shepheard**, ASN Alagha, GMB Viggiani & SK Haigh
*Department of Engineering, University of Cambridge, United Kingdom, cjs225@cam.ac.uk*

ABSTRACT: Anticipated increasing urbanisation over the coming decades is creating pressure to improve infrastructure in cities, much of which is being constructed underground in already congested subterranean environments. Tunnelling causes complex stress changes at the face of and around the tunnelling machine which can cause ground movements that propagate to the ground surface and manifest in a settlement trough above and around the tunnel axis. The movements caused by the TBM are a function of many aspects of its geometry and operation. With the exception of a handful of studies, most previous research studying tunnel construction effects have been limited in their portrayal of the tunnelling process, often regarding it as merely a partial cavity collapse. In order to more accurately model tunnel construction, a novel miniature tunnel boring machine (mini-TBM) has been designed and constructed for use in the Cambridge Geotechnical Centrifuge to model the major tunnelling processes in-flight as it progresses through dry sand. In this paper a brief overview of the mini-TBM is given and the results of an initial greenfield test are discussed. It is shown that the mini-TBM is a good model for the tunnelling process.

KEYWORDS: tunnelling, settlement, physical modelling, centrifuge, underground construction

## 1 INTRODUCTION

In an increasingly urbanised world, limited space for additional services and transport routes in cities is forcing infrastructure to be constructed underground. It is imperative for engineers to minimise the effects of damage to nearby structures caused by bored tunnelling-induced movements in soft ground. They must understand the mechanisms of the tunnelling process that cause such ground movements and predict their magnitude in order to be able to mitigate against them.

Physical modelling has been a key method in understanding many geotechnical problems. Modelling of tunnelling in soft ground has generally been split into either simplified tunnelling in a geotechnical centrifuge (Grant and Taylor 2000, Jacobsz et al. 2004, Marshall et al. 2012), which captures accurate stresses and ground movement but does not well capture the processes causing it, or complex 1g models of tunnel boring machines (TBMs) (Xu et al. 2011, Bel et al. 2015, Fang et al. 2015), which capture tunnelling processes well but are limited by unrealistic soil stresses.

A new model tunnel boring machine (mini-TBM) for use in a centrifuge has been developed at the University of Cambridge. This mini-TBM is able to 'construct' a tunnel during flight and models the major processes of tunnelling that lead to volume loss and ground movement (Mair and Taylor 1997).

This paper discusses the elements of a TBM with their effects on the surrounding ground, and how these elements have been modelled in past studies. An overview of the new mini-TBM system is presented with some preliminary results from a greenfield test in dry Hostun sand.

## 2 BACKGROUND

### *2.1 Features of a TBM*

Machines for bored tunnelling in soft ground follow a similar blueprint and consist of the following key features:

1. Cutterhead at the front to loosen and excavate the soil,
2. Pressurised working chamber which supports the tunnel face,
3. Shield, slightly conical, in which the motor and jacks are located and where the tunnel lining is constructed in stages,

And not considered part of the machine itself but part of the TBM system:

4. Tunnel lining constructed from concrete segments to support the tunnel walls.

The cutterhead of a tunnelling machine features cutting tools to break up the soil ahead of the machine and openings for the excavated material to be removed. The cutting tools tend to be similar for most types of soft ground, however the size of the openings is dependent on the type of soil being excavated. Cohesive-frictional materials such as clays have greater stability than purely frictional materials such as sand and thus TBMs designed for this type of ground can have much larger openings as they do not require the same level of mechanical face support (Berthoz et al. 2018). The percentage of the cutterhead that is open is called the opening ratio and is usually 60-80% in clays and 30-35% for sands.

The TBM shield is conical in shape to reduce squeezing from the surrounding ground. The front of the shield has a diameter around 1% smaller than the cutterhead and reduces by around 0.1-1% over its length (Ji et al. 2008, Liu et al. 2014, Schivre 2015). The tunnel lining has a smaller diameter than the rear of the shield creating the tail void; this is usually grouted as the TBM advances.

The geometry of these components and the tunnelling mechanism leads to inevitable ground movements around the TBM which can propagate around the tunnel line and damage nearby structures. Mair and Taylor (1997) identified five main sources of ground movements due to a TBM (Figure 1):

I. Stress relief at the tunnel face,
II. Overcutting causing radial soil movement,
III. Collapse of the gap between the rear of the shield and the tunnel lining (tail void collapse),
IV. Lining deflection, and
V. Long term consolidation.

Points IV and V are not directly attached to the tunnelling process and thus are not considered in this paper. Ground movement laterally due to point I can be limited by the standard practice of controlling the face pressure. Therefore, the majority of the ground movement is radial towards the centre line of the tunnel, manifested as a settlement trough at the surface (Figure 2). The settlement trough in a greenfield site can be simplified into transverse and longitudinal curves (Attewell and Hurrell 1985).

In clays, the transverse settlement trough immediately following tunnel construction is well described by a Gaussian (normal) curve. This was observed first by Martos (1958) and has been confirmed by many subsequent analyses (Peck 1969,

Schmidt 1969, Mair and Taylor 1997). The transverse settlement profile is thus described by:

$$S_z(y) = S_{x,max}\exp\left(\frac{y^2}{2i^2}\right) \quad (1)$$

where $S_{z(y)}$ is settlement on the z axis at point y, $S_{z,max}$ is the maximum settlement on the z axis (i.e. directly above the tunnel line), y is the distance from the tunnel line on the transverse (y) axis and $i$ is the trough width parameter (transverse distance from tunnel to point of inflection of Gaussian curve). The trough width parameter has a linear relationship with the depth of the tunnel (O'Reilly and New 1982):

$$i = Kz_0 \quad (2)$$

where $K$ is the dimensionless trough width parameter (0.25-0.45 for sands and gravels, 0.4-0.5 for stiff clays, and 0.6-0.7 for soft clays) and $z_0$ is the tunnel depth.

Sands do not necessarily follow the exact Gaussian curve, particularly for large volume losses where it is observed to create a much narrower trough (Attewell and Woodman 1982, O'Reilly and New 1982, Mair and Taylor 1997).

The longitudinal settlement trough in clays follows the cumulative probability curve and propagates ahead of the TBM face, parallel to the tunnel axis:

$$S_z(x) = S_z(y)\left[G\left(\frac{(x-x_i)}{i}\right) - G\left(\frac{(x-x_f)}{i}\right)\right] \quad (3)$$

where, $G(x-x_i)$ and $G(x-x_f)$ correspond to the distance between the current face position and the initial and final tunnel face positions respectively and may be determined using a probability table. It is often practical to consider the initial tunnel face position infinitely far away such that $G(x-x_i)$ is equal to 1.

Attewell and Woodman (1982) showed this to be reasonably accurate through a review of case studies. Rankin (1988) remarked that the effects of tunnelling begin to be observed ahead of the tunnel face at distances between one and two times the depth of the tunnel. It is important to note that only a maximum of 50% of the total settlement occurs above the TBM face. Indeed, the majority of the settlement is associated with the tail void collapse.

## 2.2 *Physical modelling of tunnelling*

Physical modelling of tunnelling processes in soft ground can be largely split into two categories: reduced-scale TBMs tested at 1g, and centrifuge models. Centrifuge modelling of tunnelling, due to being limited by space and power, is predominantly a heavily simplified process, whereas 1g models have the ability to be much more involved. A more complete review of the methods for modelling tunnelling is found in Meguid et al. (2008), however a brief overview is given here.

### 2.2.1 *Volume loss tunnelling models*

The severe space limitations when testing on a centrifuge have meant that modelling of tunnelling has almost exclusively modelled the induced volume loss by deflating 'balloons' around a mandrel (e.g. Grant and Taylor 2000, Jacobsz et al. 2004, Marshall et al. 2012) in 2D plane-strain conditions.

A thin rubber membrane is wrapped around the mandrel and an incompressible fluid is injected to fill the annulus. The diameter of the mandrel plus the filled membrane is that of the model-scale 'excavated' tunnel, that which the TBM excavates. During flight, this fluid is extracted until it is flush with the mandrel. The diameter of the mandrel plus the empty membrane is the diameter of the tunnel lining. The change in diameter imposes a volume loss around the model tunnel and creates the settlement trough.

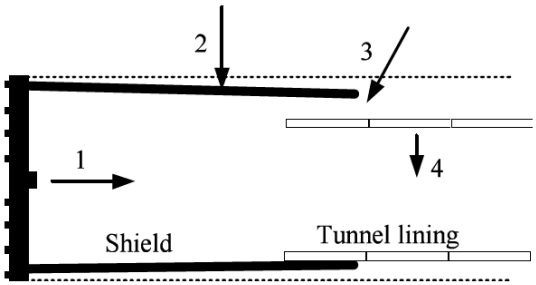


Figure 1: Sources of volume loss during tunnelling (after Mair and Taylor, 1997)

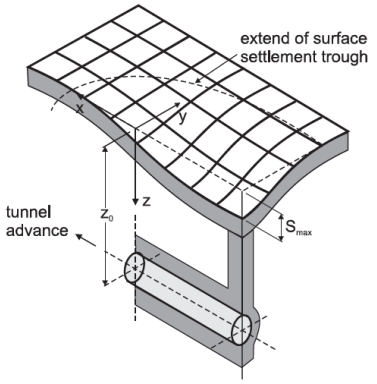


Figure 2: Ground surface settlement trough due to tunnelling (after Attewell and Hurrell 1985)

While this system does well to replicate the end result of tunnelling – a settlement trough above the tunnel line – it does not account for the three-dimensional nature of the tunnelling process and how the settlement trough develops in advance of the TBM face. This was addressed by Gue et al. (2017) in separating the model tunnel into sections and deflating the membranes in sequence. A longitudinal profile very similar to the expected cumulative probability curve was observed. This work was a significant improvement in the ability to model the development of the settlement trough more accurately, however the more complex tunnelling processes are still not included. This stepped deflation method does not account for the volume loss being created by different elements of the TBM and tunnelling process itself.

Extracting fluid from a membrane is the most common means of imposing volume loss in centrifuge models of tunnelling, however some studies have used other methods. Namely, dissolving polystyrene (Sharma et al. 2001), mechanically reducing the model tunnel diameter (e.g. Song and Marshall 2020), or using air in the 'balloon' rather than fluid.

### 2.2.2 *Reduced-scale TBMs*

Reduced scale tunnelling models have the benefit of being able to recreate the tunnelling processes that create the sources of ground movement identified by Mair and Taylor (1997) while also being repeatable and fully instrumented. However, due to the expense and size of such models, only three have been created (Bel et al. 2015): those of Xu et al. (2011), Fang et al. (2015) and Berthoz et al. (2018). Only Berthoz et al. (2018) studies the effect of tunnelling on piles. These studies have similar general setups, consisting of a large soil container into which a model TBM is driven. A summary of the main properties of these three reduced-scale tunnel boring machines is given in Table 1.

Table 1: Summary of reduced-scale TBMs tested at 1g

| Study | Soil material | Diameter (m) | Opening ratio | TBM length (m) | Tunnel cover | Notes |
|---|---|---|---|---|---|---|
| Xu et al. (2011) | Silty clay | 0.4 | 40% | 2.0 | 0.8-1.6 | Does not model overcut or tail void. |
| Fang et al. (2015) | Sandy soil | 0.52 | 54.5% | 0.85 | 0.55 | Overcut 6mm, 20mm tail void. |
| Berthoz et al. (2018) | Sand (Hostun HN31) | 0.55 | 35% | 2.0 | 1.2 | Does not model tail void (max penetration 1m). |

While these models manage to capture much of the complexity of the tunnel boring process and have produced some useful results, some limitations do apply. For example, the soil container used by Fang et al. (2011) was not sufficiently wide enough to allow the full transverse trough to develop and thus some interference from the container walls is observed. It must also be noted that not all of these models capture the full complexity of the tunnelling process as the models of Xu et al. (2011) and Berthoz et al. (2018) do not include the tail void, and none of the three have a conical shield.

Before the creation of the miniature-TBM presented in this paper, only Nomoto et al. (1999) had created a reduced-scale TBM for use in a centrifuge. This is a complex system consisting of three tubes: an outer shield tube with 100mm diameter, a

middle lining tube with diameter 96mm, and a central tube for extraction of excavated soil which houses a screw auger. Dry Toyoura sand with density 70% was used. A centrifugal acceleration of 25g was used, modelling a tunnel of 2.5m diameter at prototype scale.

The tunnelling process was modelled in a two-part procedure. First the three tubes were driven into the soil container, with sand being extracted by the screw auger. When the model TBM reached the desired location the drive process was stopped and then the outermost shield tube was removed to simulate the creation of the tail void.

This study by Nomoto et al. (1999) was possibly the closest to being able to fully model the tunnelling process and its effect on soil; not only did it account for some of the features of a TBM and modelled the three-dimensional trough progression as with the 1g models, but by using the centrifuge realistic soil stresses were able to be modelled. However, this TBM model was limited in many ways physically as it did not include an overcut or shield conicity. Also, as the tunnelling process was modelled in two halves, with the tail void being created separately to the advance of the machine it could be improved upon if the whole process were continuous.

By accounting for most of the elements of a TBM which cause ground movements and its suitability for use in a centrifuge, the new mini-TBM described in this paper aims to create the most accurate physical model of the tunnelling process yet.

## 3 NEW TUNNELLING MODEL

The mini-TBM was developed at the University of Cambridge over two years to model the process of shield tunnelling in soft ground. The design encompasses the overcut at the head of the shield, the conical shape of the shield, and the change in diameter between the rear of the shield and the tunnel lining.

### 3.1 *Geometry and structure of mini-TBM*

A more complete discussion of the design of the geometry of the mini-TBM can be found in Shepheard et al. (2021), however a brief overview is given here as some dimensions have been changed. The mini-TBM is designed in a modular fashion such that individual components may be changed simply. Therefore the primary components of the mini-TBM are the cutterhead, the working chamber, the 'shield' collar and the lining tube. Figure 3 shows a drawing of the mini-TBM system and Figure 4 is a photograph of the mini-TBM.

The lining tube has an outer diameter of 76.2mm and thickness of 3mm. It represents the walls of the completed sections of a tunnel. At the front of the lining tube, the outer diameter is reduced by 1.5mm to allow the 100mm long shield collar to slot onto the tube.

The shield collar has a conical cross section to model the typical conical or telescopic design of TBM shield machines. The diameter reduces from 77mm at the front to 76.2mm at the rear. No tail void is modelled at the rear of the shield in this iteration of the mini-TBM. It was decided that this was allowable at this stage in development as in modern tunnelling processes, this is usually well filled by a grouting process to greatly limit the effect of tail void collapse.

The cutterhead sits ahead of the shield with an opening ratio of 40% and an overcut of around 1%. The diameter of the cutterhead is 78mm and it has a thickness of 10mm. Inside the front of the shield is a conical brass working chamber to guidethe excavated soil to a 40mm diameter screw auger for extraction. The screw auger is housed inside a smaller tube to contain the removed soil.

The mini-TBM is driven by two servo motors attached respectively to a 1D actuator for the advance thrust and the screw

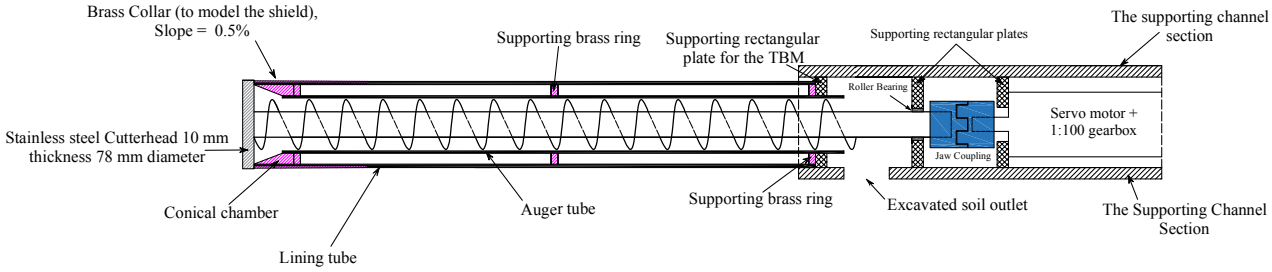


Figure 3: Schematic of the mini-TBM

auger for the rotational excavation. The motors are controlled independently such that the advance speed may be balanced with the excavation rate in order to control the overall volume loss. The cutterhead is attached to the auger and they rotate in tandem.

Figure 4: Photograph of the mini-TBM attached to the actuator.

### 3.2 *Experiment setup*

The mini-TBM has been designed for use in the Cambridge geotechnical centrifuge. The mini-TBM is driven into a strong box of dry Hostun sand with an approximate relative density of 55% at a depth of 2.5*D* where *D* is the diameter of the cutterhead.

The interior of the strong box has a width of 780mm, depth 460mm and height 374.5mm. A hole in the front of the box for the mini-TBM to enter is located at a height of 139.5mm from the base.

Due to the change in diameter of the mini-TBM from the front of the cutterhead to the rear of the shield and the requirement for the entry hole to have a tight fit to prevent the escape of sand, these elements are located inside the box at the start of the test. Thus, the cutterhead is located 110mm from the front wall of the strong box at the start of the test. The distance the mini-TBM is able to advance is limited to 280mm by the strike of the 1D actuator.

LVDTs were used for measurement of the ground surface displacement. Figure 5 shows locations of the LVDTs. They were only placed on one half of the surface as the other half was monitored by a photogrammetry system. The data from the photos has not yet been analysed, so for the purposes of this paper the ground movements are considered symmetrical from the LVDTs.. Symmetry about the tunnel axis is assumed for a simple analysis of the ground surface movement in this paper.

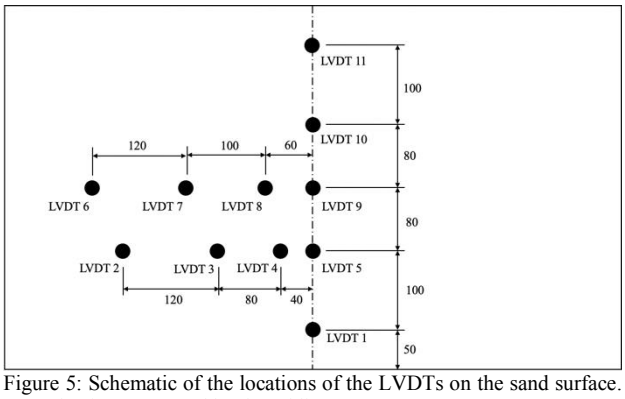


Figure 5: Schematic of the locations of the LVDTs on the sand surface. Tunnel axis represented by dotted line.

### 3.3 *Test procedure*

While the mini-TBM system will be designed to be used at up to 50g, this experiment was performed under 20g to account for the current limitations of the system when used in sand. Thus this paper models the construction of a 'micro tunnel' with a diameter of 1.5m.

Some advance rate/rotation rate balancing issues were encountered at the start of the test leading initially to some heave. This was overcorrected and resulted in over-excavation which was greater than what was initially aimed for in this test. Nevertheless, as this paper is intended to show a proof of concept for the mini-TBM, the results are still considered useful in this regard. A final advance rate of 6.2mm/min with a rotational speed of 1.15rpm was decided upon from a distance of around 15mm from the mini-TBM face start position and was held constant through the remainder of the test.

## 4 TEST RESULTS

The results in Figures 6 to 9 from the LVDTs on the sand surface show that the mini-TBM produces a settlement trough that is very similar to that which would be expected from past studies. As discussed above, the transverse settlement troughs presented in this paper are constructed from the mirrored data from LVDTs on one half of the model surface.

### 4.1 *Longitudinal settlement*

The longitudinal settlement profile along the tunnel axis at LVDT locations 5, 9, 10 and 11 relative to the position of the face of the mini-TBM is shown in Figure 6.

It can be seen in Figure 6a that the profiles appear to never reach a steady state point at which there is no more settlement. This is possibly due to 'heave' caused by the friction between the lining tube and the sand around it. In actual tunnelling, the shield moves separately to the lining which, once constructed, does not move. For simplicity in this model, the 'tunnel lining' currently moves with the shield and thus may be able to effectively 'drag' some surrounding sand along with it. This, along with boundary effects at the back of the box causes the 'heave'. The mini-TBM, limited by the strike of the actuator, does not ever reach LVDT 11, so this may be used as a simple normaliser for the data. This has been performed and is shown in Figure 6b. This adjustment suggests that LVDT 5 has completed its full settlement profile, and LVDT 9 is close to completion at the end of the experiment but is limited by the distance the mini-TBM can travel.

Figure 6b shows that the ground surface experiences little to no movement until the face of the mini-TBM is within around 0.5D of the location. The vast majority of ground movement takes place between the point at which the face of the mini-TBM is under a point and 1D past. This corresponds with the findings of previous studies and is consistent with the expected behaviour of sands in particular. In clays, these troughs would be expected to be much longer, with ground movement seen further ahead of the mini-TBM face and the maximum settlement achieved further after the face passage.

There is also a difference in observed total volume loss when comparing the results from LVDT 5 and LVDTs 9 and 10. LVDT 5 shows a maximum settlement corresponding to a volume loss of around 14.5%, whereas LVDT 9 shows a volume loss of just over 10% (LVDT 10 has not developed a complete enough settlement trough to calculate the maximum volume loss). This is due to some advance/rotation balancing issues throughout the test as mentioned above. Therefore, when considering transverse movements, the result from the second row of LVDTs 6 to 9 is arguably more reliable as the first row was positioned very close to the face of the mini-TBM while the balancing issues were being addressed. All ground movement observed in the second transverse row of LVDTs 6 to 9 occurred after the final advance parameters had been established. The observed maximum settlement relates to about 80mm of settlement at prototype scale.

It can be seen in Figure 6 also that the settlement curves from LVDTs 9 and 10 map onto each other very well. This suggests that once the advance parameters had been established, the tunnelling process was consistent.

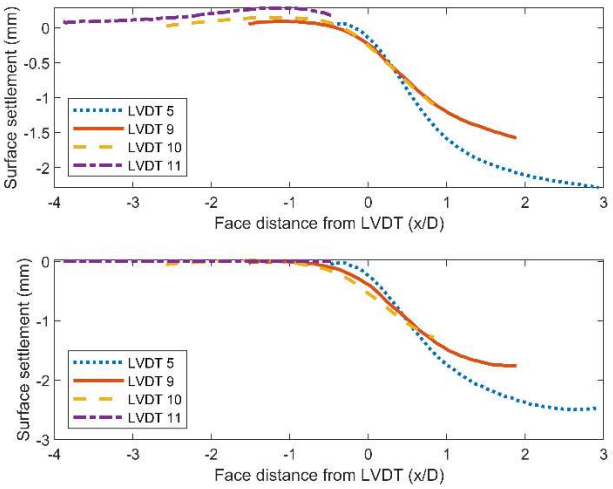


Figure 6: Longitudinal ground movement profiles for the LVDTs on the tunnel axis relative to tunnel face position (a) raw data and (b) normalised with respect to LVDT 11.

### 4.2 *Transverse settlement*

Figures 7 and 8 show the measurement results for the ground surface displacement in the transverse direction at the end of the test compared to a Gaussian curve. It can be seen that the troughs created in the sand are narrower than the standard Gaussian curves, which is to be expected from past studies as sands tend to create a chimneying effect, however the general shape of the transverse settlement troughs fits well with the literature.

The development of the transverse settlement trough on the line of LVDTs 6 to 9 is shown in Figure 9. It can be seen that there is some heave before and as the face of the mini-TBM gets close to the line of LVDTs, but this is minimal, and as the mini-TBM passes beneath and past the line, the settlement trough develops as would be expected with the majority of the movement when the relative position of the mini-TBM face is between 0D and 1.5D. This also corresponds to the longitudinal ground surface settlement profile shown in Figure 6.

## 5 CONCLUSIONS

This paper presented an overview of the design of a new mini-TBM for use in a geotechnical centrifuge to better model in-flight the main processes of tunnelling which cause ground surface movement.

From a preliminary experiment at a centrifugal acceleration of 20g, it has been shown that the Cambridge mini-TBM produces ground settlement profiles in the longitudinal and transverse directions that are very similar to those previously reported in past studies. Hence, it is believed that the mini-TBM is a good model for the tunnelling process and is an improvement on past reduced-scale physical models, as it allows for the accurate modelling of field stresses while also including more of the complexities of the tunnelling process.

Further work will be undertaken using the mini-TBM, both in dry sand and soft clay. The reaction of model piles will also be studied.

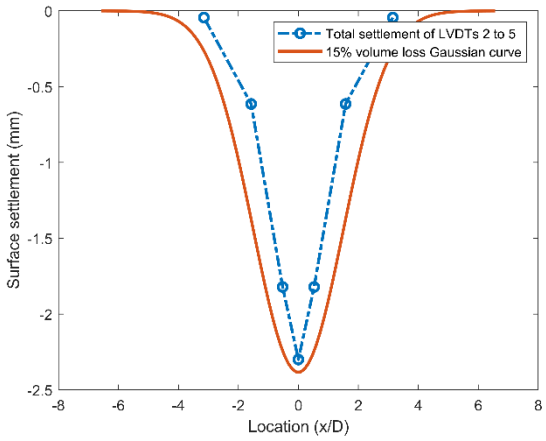


Figure 7. Transverse ground settlement from LVDTs 2 to 5 at end of test compared to 15% volume loss standard Gaussian curve.

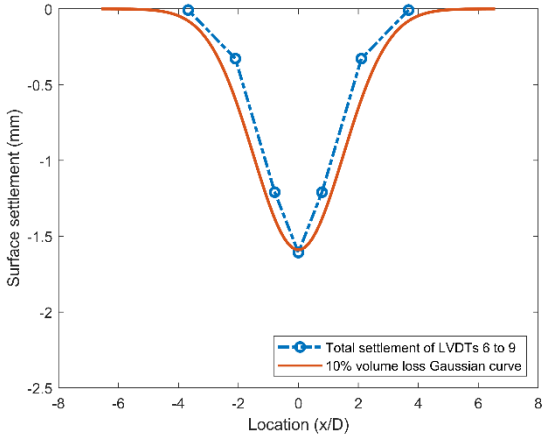


Figure 8. Transverse ground settlement from LVDTs 6 to 9 at end of test compared to 10% volume loss standard Gaussian curve.

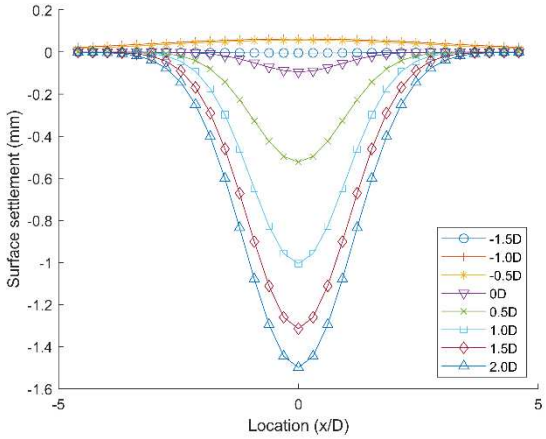


Figure 9: Transverse profiles of ground movement on the line of LVDTs 6 to 9 as the mini-TBM face advances towards and past the cross section.

## 6 REFERENCES

Attewell, P.B., and Hurrell, M.R. 1985. Settlement Development Caused By Tunnelling in Soil. Ground Engineering, **18**(8): 17–20.

Attewell, P.B., and Woodman, J.P. 1982. Settlement and Its Derivitives Caused By Tunnelling in Soil. Ground Engineering, **2**(8): 13–22.

Bel, J., Branque, D., Wong, H., Viggiani, G., and Losacco, N. 2015. Experimental study on a 1g reduced scale model of TBM: impact of tunnelling on piled structures. Geotechnical Engineering for Infrastructure and Development: XVI European Conference on Soil Mechanics and Geotechnical Engineering,: 413–418. doi:10.1680/ecsmge.60678.

Berthoz, N., Branque, D., Wong, H., and Subrin, D. 2018. TBM soft ground interaction: Experimental study on a 1 g reduced-scale EPBS model. Tunnelling and Underground Space Technology, **72**: 189–209. Pergamon. doi:10.1016/j.tust.2017.11.022.

Fang, Y., Yang, Z., Cui, G., and He, C. 2015. Prediction of surface settlement process based on model shield tunnel driving test. Arabian Journal of Geosciences, **8**(10): 7787–7796. doi:10.1007/s12517-015-1800-0.

Grant, R.J., and Taylor, R.N. 2000. Tunnelling-induced ground movements in clay. Proceedings of the Institution of Civil Engineers, Geotechnical Engineering, **143**(1): 43–55. doi:10.1680/geng.2000.143.1.43.

Gue, C.Y., Wilcock, M.J., Alhaddad, M.M., Elshafie, M.Z.E.B., Soga, K., and Mair, R.J. 2017. Tunnelling close beneath an existing tunnel in clay-perpendicular undercrossing. Geotechnique, **67**(9): 795–807. doi:10.1680/jgeot.SiP17.P.117.

Jacobsz, S.W., Standing, J.R., Mair, R.J., Hagiwara, T., and Sugiyama, T. 2004. Centrifuge Modelling of Tunnelling Near Driven Piles. Soils and Foundations, **44**(1): 49–56. doi:10.3208/sandf.44.49.

Ji, Q.Q., Huang, Z.H., and Peng, X.L. 2008. Analysis on influence of conicity of extra-large diameter mixed shield machine on surface settlement. *In* The ShanghaiYangtze River Tunnel: Theory, Design and Construction. *Edited by* R. Huang. Taylor & Francis, Shanghai, China. pp. 237–274.

Liu, C., Zhang, Z., and Regueiro, R.A. 2014. Pile and pile group response to tunnelling using a large diameter slurry shield - Case study in Shanghai. Computers and Geotechnics, **59**(October): 21–43. Elsevier Ltd. doi:10.1016/j.compgeo.2014.03.006.

Mair, R.J., and Taylor, R.N. 1997. "Theme Lecture: Bored tunnelling in the urban environment," Plenary Session 4. *In* 14th International conference on soil mechanics and foundation engineering. pp. 2353–2385. Available from http://ci.nii.ac.jp.sci-hub.org/naid/80011078002.

Marshall, A.M., Farrell, R., Klar, A., and Mair, R. 2012. Tunnels in sands: the effect of size, depth and volume loss on greenfield displacements. Géotechnique, **62**(5): 385–399. doi:10.1680/geot.10.P.047.

Martos, F. 1958. Concerning an approximate equation of the subsidence trough and its time factors. *In* International Strata Control Congress. pp. 191–205.

Meguid, M.A., Saada, O., Nunes, M.A., and Mattar, J. 2008. Physical modeling of tunnels in soft ground: A review. Tunnelling and Underground Space Technology, **23**(2): 185–198. doi:10.1016/j.tust.2007.02.003.

Nomoto, T., Imamura, S., Hagiwara, T., Kusakabe, O., and Fujii, N. 1999. Shield tunnel construction in centrifuge. Journal of Geotechnical and Geoenvironmental Engineering, **4**(125): 289–300. doi:10.1061/(ASCE)1090-0241(1999)125:4(289).

O'Reilley, M.P., and New, B.M. 1982. Settlements above tunnels in the United Kingdom - their magnitude and prediction. *In* Tunnelling '82: Pro- ceedings of the 3rd International Symposium. *Edited by* M.J. Jones. Institution of Mining and Metallurgy, London. pp. 173–181.

Peck, R.B. 1969. Deep excavations and tunnelling in soft ground. *In* 7th International Conference on Soil Mechanics and Foundation Engineering, Mexico City, Mexico. pp. 225–290.

Rankin, W.J. 1988. Ground movements resulting from urban tunnelling: predictions and effects. Geological Society, London, Engineering Geology Special Publications, **5**(1): 79–92. doi:10.1144/gsl.eng.1988.005.01.06.

Schivre, M. 2015. Frejus highway tunnel. Available from https://www.ethz.ch/content/dam/ethz/special-interest/baug/igt/tunneling-dam/kolloquien/2015/schivre_prasentation.pdf [accessed 21 May 2019].

Schmidt, B. 1969. Settlements and ground movements associated with tunnelling in soil. University of Illinois, Urbana.

Sharma, J.S., Bolton, M.D., and Boyle, R.E. 2001. A New Technique for Simulation of Tunnel Excavation in a Centrifuge. Geotechnical Testing Journal, **24**(4): 343–349. doi:10.1520/GTJ11131J.

Shepheard, C.J., Alagha, A.S.N., Viggiani, G.M.B., and Haigh, S.K. 2021. A miniature EPB TBM for use in a geotechnical centrifuge. Geotechnical Aspects of Underground Construction in Soft Ground,: 415–420. doi:10.1201/9780429321559-54.

Song, G., and Marshall, A.M. 2020. Centrifuge modelling of tunnelling induced ground displacements: pressure and displacement control tunnels. Tunnelling and Underground Space Technology, **103**(May): 103461. Elsevier. doi:10.1016/j.tust.2020.103461.

Xu, Q., Zhu, H., Ding, W., and Ge, X. 2011. Laboratory model tests and field investigations of EPB shield machine tunnelling in soft ground in Shanghai. Tunnelling and Underground Space Technology, **26**(1): 1–14. doi:10.1016/j.tust.2010.09.005.